TLR9 induces colitis-associated colorectal carcinogenesis by regulating NF-κB expression levels

QINGTIAN LUO[1,2], LING ZENG[1], CHAOTAO TANG[1], ZHENDONG ZHANG[3], YOUXIANG CHEN[1] and CHUNYAN ZENG[1]

[1]Department of Gastroenterology, The First Affiliated Hospital of Nanchang University, Nanchang, Jiangxi 330006; [2]Department of Gastroenterology, The Affiliated Ganzhou Hospital of Nanchang University, Ganzhou, Jiangxi 341000; [3]Department of Pathology, The First Affiliated Hospital of Nanchang University, Nanchang, Jiangxi 330006, P.R. China

Received September 13, 2019; Accepted July 8, 2020

DOI: 10.3892/ol.2020.11971

Abstract. Chronic colorectal inflammation has been associated with colorectal cancer (CRC); however, its exact molecular mechanisms remain unclear. The present study aimed to investigate the effect of Toll-like receptor 9 (TLR9) on the development of colitis-associated CRC (CAC) through its regulation of the NF-κB signaling pathway. By using a CAC mouse model and immunohistochemistry, the present study discovered that the protein expression levels of TLR9 were gradually upregulated during the development of CRC. In addition, the expression levels of TLR9 were revealed to be positively correlated with NF-κB and Ki67 expression levels. In vitro, inhibiting TLR9 expression levels using chloroquine decreased the cell viability, proliferation and migration of the CRC cell line HT29, and further experiments indicated that this may occur through downregulating the expression levels of NF-κB, proliferating cell nuclear antigen and Bcl-xl. In conclusion, the findings of the present study suggested that TLR9 may serve an important role in the development of CAC by regulating NF-κB signaling.

Correspondence to: Professor Youxiang Chen or Dr Chunyan Zeng, Department of Gastroenterology, The First Affiliated Hospital of Nanchang University, 17 Yongwaizheng Street, Nanchang, Jiangxi 330006, P.R. China
E-mail: chenyx102@126.com
E-mail: zcy896@163.com

Abbreviations: AIF, acute inflammation; AOM, azoxymethane; CAC, colitis-associated colorectal cancer; CIF, chronic inflammation; CRC, colorectal cancer; DAI, disease activity index; DSS, dextran sodium sulfate; IBD, inflammatory bowel disease; IECs, intestinal epithelial cells; IHC, immunohistochemistry; PCNA, proliferating cell nuclear antigen; TLR9, Toll-like receptor 9; UC, ulcerative colitis

Key words: colitis-associated CRC, AOM, DSS, TLR9, NF-κB

Introduction

The number of patients with colorectal cancer (CRC) worldwide is increasing annually, with an incidence rate of 6.1% in 2018 (1). Chronic inflammation is the leading cause of immune cell infiltration and proliferation, and it has been suggested to be a high-risk factor for colitis-associated CRC (CAC) (2). Inflammatory bowel disease (IBD), which encompasses both ulcerative colitis (UC) and Crohn's disease, was established as an important precursor to CRC (3,4). For example, the incidence of IBD-associated CRC in patients with UC was reported to have a cumulative risk rate of 2% at 10 years, 8% at 20 years and 18% at 30 years of disease duration (3). Therefore, further *in vivo* studies are required for researchers to gain an improved understanding of the molecular mechanisms of CAC, which may provide more exact molecular targets for the diagnosis and treatment of CAC during the early stages.

Toll-like receptor (TLR)9, a member of the TLR family, is located in the cytoplasm and intracellular endosomes, and can be activated by unmethylated bacterial CpG DNA (5). The activation of the TLR9 signaling pathway induces a Type 1 T helper cell immune response and stimulates the proliferation of B cells, thus protecting the host from external microbial invasion (6-9). Multiple studies have revealed that abnormal TLR9 expression levels were involved in the pathogenesis and progression of UC (10,11). In addition, abnormal expression levels of TLR9 were also identified during the tumorigenesis and development of CRC (12-15).

NF-κB is an important transcription factor involved in various biological processes, including inflammatory reactions, immune responses, apoptosis and proliferation (16). In fact, NF-κB is regarded as a molecular hub that links inflammation and cancer (17). It was previously suggested that NF-κB may serve an important role in colorectal carcinogenesis by regulating matrix metalloproteinase-9 expression (18-20). Previous studies have revealed that TLR9 was related to the biological characteristics of various types of cancer, including bladder, lung and prostate cancer, such as cell proliferation, invasion, tumor growth and progression (21-24). In fact, one previous study reported that TLR9 regulated the expression levels of interleukin (IL)-6 through the myeloid differentiation primary response protein MyD88 (MyD88)/NF-κB signaling

pathway in myeloid cells to promote tumor recurrence after irradiation, including in melanoma, bladder carcinoma and colorectal carcinoma (25).

The current study aimed to investigate the effect of TLR9 on the development of CAC through its regulation of the NF-κB signaling pathway. Owing to the synergistic effects of azoxymethane (AOM), a tumor-inducing agent, and dextran sodium sulfate (DSS), a tumor-promoting agent (26), the present study established CAC model mice by co-administering AOM and DSS to analyze the expression levels of TLR9, NF-κB and Ki67 in CAC tissues.

Materials and methods

Reagents and antibodies. AOM (cat. no. A5486) and chloroquine (TLR9 inhibitor; cat. no. C6628-25G) were obtained from Sigma-Aldrich; Merck KGaA. DSS (cat. no. 0216011080-100G) was purchased from MP Biomedicals, LLC. Anti-TLR9 (cat. no. ab134368) and anti-MyD88 (cat. no. ab135693) primary antibodies were obtained from Abcam. Anti-NF-κB (NF-κB p65; cat. no. 8242S), anti-Bcl-xl (cat. no. 2764) and anti-Ki67 (cat. no. 9449S) primary antibodies were obtained from Cell Signaling Technology, Inc. The anti-proliferating cell nuclear antigen (PCNA; cat. no. sc-56) primary antibody was obtained from Santa Cruz Biotechnology, Inc. and the anti-GAPDH (cat. no. TA309157) primary antibody was obtained from OriGene Technologies, Inc. Horseradish peroxidase secondary goat anti-rabbit (cat. no. ZB-2301) and goat anti-mouse (cat. no. ZB-2305) antibodies, used for western blotting, and goat anti-mouse/rabbit antibodies (cat. no. TA130001/TA130015) used for immunohistochemistry (IHC) were obtained from OriGene Technologies, Inc.

Cell lines and culture. The human CRC cell line HT29 was obtained from the American Type Culture Collection and cultured in McCoy's 5A (Modified) medium (Gibco; Thermo Fisher Scientific, Inc.), supplemented with 10% FBS (Gibco; Thermo Fisher Scientific, Inc.), 50 mg/ml penicillin and 50 mg/ml streptomycin, maintained in a humidified atmosphere of 5% CO_2 at 37˚C.

Western blotting. Cells were lysed in RIPA lysis buffer (Beijing Solarbio Science & Technology Co., Ltd.) at 4˚C for 30 min. The protein concentration was measured following centrifugation at 12,000 x g for 15 min at 4˚C and quantified using a bicinchoninic acid protein assay kit (Beijing Solarbio Science & Technology Co., Ltd.). An equal amount of protein (50 μg/lane) was separated via 10% SDS-PAGE and electrophoretically transferred onto polyvinylidene difluoride membranes (EMD Millipore). The membranes were blocked with 5% skimmed milk for 2 h at room temperature and were subsequently incubated overnight at 4˚C with the following primary antibodies: Anti-TLR9 (1:1,000), anti-NF-κB (1:1,000), anti-Bcl-xl (1:1,000), anti-PCNA (1:1,000), anti-MyD88 (1:500) and anti-GAPDH (1:1,000). Following the primary antibody incubation, the membranes were washed 3 times with PBS for 10 min each and incubated with the corresponding goat anti-rabbit or goat anti-mouse secondary antibodies at 4˚C for 4 h. Protein bands were visualized using an ECL reagent (Thermo Fisher Scientific, Inc.) on a Gel Doc XR+ system (Bio-Rad Laboratories, Inc.) and analyzed using Image Lab version 2.0 software (Bio-Rad Laboratories, Inc.).

Wound healing assay. A wound healing assay was performed to analyze the cell migratory ability. Briefly, HT29 cells ($3x10^5$/well) were seeded into six-well plates and cultured to 90-100% confluence. Subsequently, a 200-μl pipette tip was used to scratch a wound in the cell monolayer. Fresh serum-free McCoy's 5A (Modified) medium containing different concentrations of chloroquine (0, 15 or 25 μg/ml) was added to each well and cultured for 48 h in a humidified atmosphere of 5% CO_2 at 37˚C. Images of each well were captured at 0 and 48 h using a light phase contrast microscope (Olympus, ZKX-41; Olympus Corporation) with a magnification of x100. The wound-healing areas were assessed using ImageJ 1.52a software (National Institutes of Health). The migratory rate of cells = (wound area at 0 h-wound area at 48 h)/area at 0 h.

Colony formation assay. HT29 cells ($1.2x10^5$/well) were cultured in 6-well plates for 48 h in medium containing different concentrations of chloroquine (0, 15 or 25 μg/ml) at 37˚C, and then seeded into 6-cm cell culture dishes (500 cells/dish) and incubated in complete medium at 37˚C. After 14 days, the cells were fixed with 4% paraformaldehyde for 15 min and stained with 0.1% crystal violet for 30 min, both at room temperature. The number of colonies, defined as >50 cells/colony, was counted manually using a light microscope with a magnification of x100. Relative colony number = number of colonies in observed group/number of colonies in control group. All of the experiments were repeated ≥3 times.

Cell viability assay. The viability of HT29 cells was analyzed using an MTT assay. Briefly, HT29 cells were seeded at a density of 5,000 cells/well in a 96-well plate and treated for 24, 48 or 72 h with chloroquine (0, 100, 125 or 150 μg/ml) at 37˚C and then analyzed using an MTT assay as previously described (27).

Animal studies. All animal experiments were approved by the ethics committee of The First Affiliated Hospital of Nanchang University (Nanchang, China). A total of 144 female BALB/c mice (weight, 20-24 g; age, 8-10 weeks) were obtained from Beijing Vital River Laboratory Animal Technology Co. Ltd. (Laboratory Animal License no. SCXK 2017-0012). The animals were maintained with a normal diet and tap water ad libitum at a temperature of 23±2˚C and a relative humidity of 40-60%, and artificially illuminated on an approximate 12 h light/dark cycle at the Animal Care Facility in the Medical College of Nanchang University. All of the mice experiments were approved by the Animal Care and Use Committee of Nanchang University. The total experiment lasted for 23 weeks. The mice were divided into four groups (36 mice/group): i) Group A (AOM + DSS), which was intraperitoneally injected without anesthesia with 10 mg/kg AOM once on the first day, followed by 3% DSS given in the drinking water for 1 week and then 2 weeks of distilled water (one cycle), which was repeated for two additional cycles; ii) Group B (AOM), which was intraperitoneally injected with 10 mg/kg AOM once on the first day and provided with distilled drinking water during weeks 0-9; iii) Group C (DSS), which was treated with DSS

as described for group A but without the AOM treatment; and iv) Group D (blank control), which received neither DSS nor AOM treatment and was provided with distilled drinking water for the first 9 weeks. All the mice were provided with a normal diet and tap water during weeks 10-23 (Fig. 1A).

The disease activity index (DAI) was evaluated at the end of the experiment using the numerical system described by Tian *et al* (28). The DAI parameters included total body weight loss (0, none; 1, 1-5%; 2, 5-10%; 3, 10-20%; 4, >20%), stool consistency (0, well-formed pellets; 2, loose stool; 4, diarrhoea) and the presence of fecal occult blood (0, negative; 2, positive; 4, gross bleeding).

Several mice were randomly sacrificed at certain times points following AOM injection (the 1st, 2nd, 3rd, 6th, 9th, 12th, 18th and 23rd weeks). Six mice were sacrificed at weeks 1, 2, 3 and 6, one mouse was sacrificed at week 9 and four mice were sacrificed at weeks 12 and 18 in each group. Additionally, six mice in group D were randomly sacrificed at week 0 as control. All remaining mice were sacrificed at week 23. After the large bowels were resected and washed with PBS, they were carefully examined, photographed and fixed in 10% formalin at room temperature for 24 h. Further histological examinations were subsequently performed.

Histopathological analysis and immunohistochemistry (IHC). Paraffin-embedded colorectal sections (5-μm-thick) were stained with hematoxylin for 2 min and eosin for 5 min at room temperature to analyze the degree of inflammation using a light microscope with magnifications of x40 and x100. Briefly, the severity of inflammation, the thickness of inflammation the severity of epithelial damage and the extent of the lesions were each graded from 0 to 3 by two investigators who were blinded to the treatment groups, as previously described (29,30). The severity of inflammation was adapted from the grading system developed by Truelove and Richards (31,32) as follows: i) Grade 0, no neutrophil infiltration in the lamina propria; ii) Grade I, infiltration of a small number of neutrophils [<10 cells/high power field (HPF)] in the lamina propria, involving a few crypts; iii) Grade II, obvious neutrophil infiltration in the lamina propria (10-50 cells/HPF), involving >50% of the crypts; iv) Grade III, infiltration of neutrophils (>50 cells/HPF) in the lamina propria with crypt abscess; and v) Grade IV, obvious acute inflammation in the lamina propria with ulcer formation. Grade I was classified as mild, grade II was classified as moderate, and grades III and IV were classified as severe. The severity of inflammation ranged from 0 to 3 (0, no inflammation; 1, mild; 2, moderate; 3, severe), the thickness of inflammation ranged from 0 to 3 (0, no inflammation; 1, mucosa; 2, mucosa plus submucosa; 3, transmural), the severity of epithelial damage ranged from 0 to 3 (0, intact epithelium; 1, disruption of architectural structure; 2, erosion; 3, ulceration) and the extent of lesions ranged from 0 to 3 (0, no lesions; 1, punctuate; 2, multifocal; 3, diffuse).

IHC was performed as described in our previous study (33). Colorectal tissues were fixed in 10% formalin for 24 h at room temperature. Formalin-fixed and paraffin-embedded tissue blocks were cut into 5-μm-thick sections and mounted on glass slides. Slides were heated in an oven at 70˚C for 90 min and deparaffined in xylene twice for 10 min each at room temperature, rehydrated in a descending ethanol series (100, 95 and 85% ethanol for 5 min each at room temperature) and incubated in 3% H_2O_2 for 8 min at room temperature to block endogenous peroxidase. Antigen retrieval was performed by heating in a microwave at 100˚C in sodium citrate buffer (3 mM, pH 6.0) for 15 min. Slides were blocked with 5% bovine serum albumin (Beijing Solarbio Science & Technology Co., Ltd.) for 1 h at room temperature to block non-specific antibody binding and incubated overnight at 4˚C with the following primary antibodies: Anti-TLR9 (1:400), anti-NF-κB (1:200) and anti-Ki67 (1:100). Following the primary antibody incubation, the sections were washed three times with PBS and incubated with horseradish peroxidase secondary goat anti-mouse/rabbit antibodies (ready to use) at 37˚C for 30 min. The sections were stained with 3,3'-diaminobenzidine at room temperature; the duration of staining was based on the staining observed under a light microscope with a magnification of x100, and the reaction was terminated when the staining was yellowish-brown. The sections were then counterstained with hematoxylin for 1 min at room temperature. The slides were observed under a light microscope with a magnification of x100. The widely accepted German semi-quantitative scoring system (34,35) was used to determine the staining intensity and area of staining, according to the recommendations of Remmele and Stegner (36). Each specimen was assigned a score according to the intensity of the nucleic, cytoplasmic and/or membrane staining (no staining, not detected=0; weak staining, light yellow=1; moderate staining, yellowish brown=2; strong staining, brown=3) and the extent of stained cells (no staining, 0; 1-24%, 1; 25-49%, 2; 50-74%, 3; 75-100%, 4). The final immunoreactive score was determined by multiplying the intensity score with the extent of stained cells score, ranging from 0 (the minimum) to 12 (the maximum).

Co-immunoprecipitation assay. HT29 cells were lysed in RIPA lysis buffer (Beijin Solarbio Science & Technology Co., Ltd.) at 4˚C for 30 min. Whole-cell lysates were pelleted via centrifugation at 10,000 x g for 10 min at 4˚C. The supernatant was incubated with an anti-TLR9 antibody (1:200) or goat anti-mouse IgG (1:200; cat. no. ZB-2305; OriGene Technologies, Inc.), together with protein A/G PLUS-Agarose beads (Santa Cruz Biotechnology) at 4˚C overnight. The beads were washed three times with the non-lubrol lysis buffer at 2,500 x g centrifugation for 5 min at 4˚C, then subjected to SDS-PAGE and subsequent western blotting analysis as aforementioned. Whole cell lysate was used as a control.

Statistical analysis. Statistical analysis was performed using SPSS 20.0 software (IBM Corp.). The data are presented as the mean ± SD. All experiments were performed at least in triplicate. A one-way ANOVA followed by a Tukey's post hoc test was used to determine the statistical differences between >2 groups, whereas an unpaired Student's t-test were used to determine the statistical differences between 2 groups. A Spearman's rank correlation test was used to determine the correlation between the expression levels of TLR9, NF-κB and Ki67 in CRC tissues. $P<0.05$ was considered to indicate a statistically significant difference.

Results

Construction of the CAC model mice. In groups A (AOM + DSS) and C (DSS), the body weights of the mice decreased with

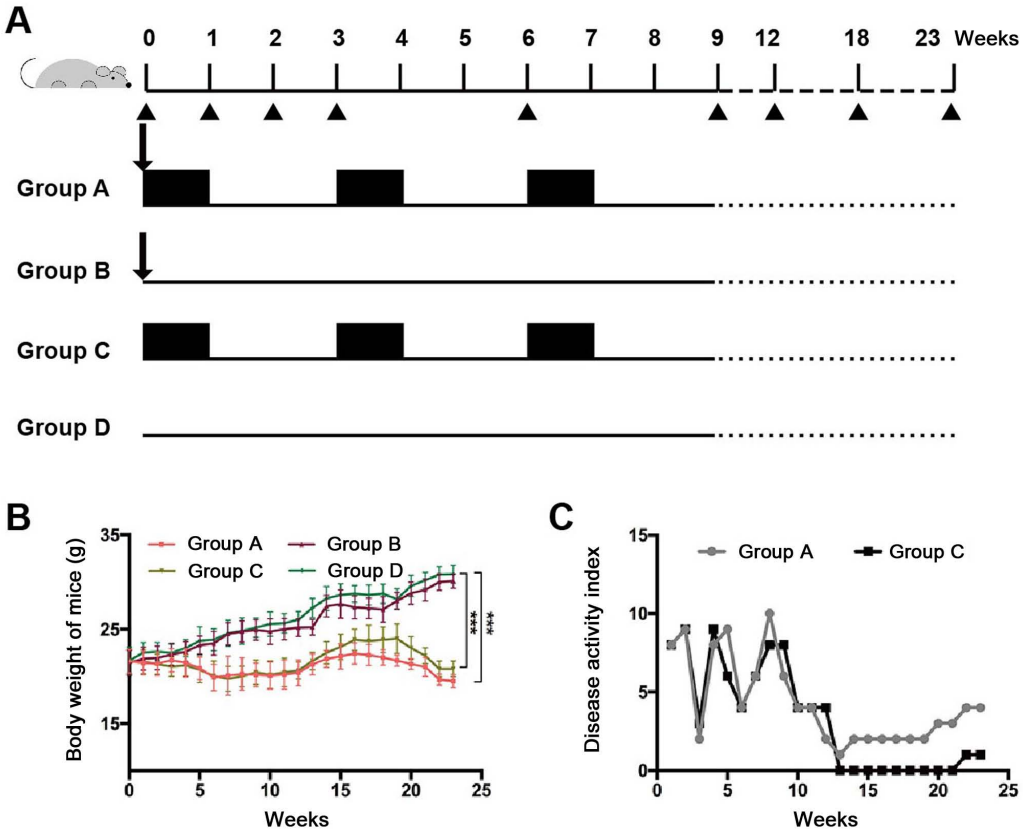

Figure 1. Construction of the colitis-associated-colorectal cancer model in mice. (A) Schematic diagram of the experimental protocol for colitis-associated colorectal cancer model mice in groups A-D. Arrow indicates 10 mg/kg azoxymethane administration via intraperitoneal injection; black square indicates administration of 3% dextran sodium sulfate in drinking water for 1 week; continuous line indicates duration fed a normal diet and distilled water; dotted line indicates duration fed a normal diet and tap water; and triangle indicates timepoint of sacrifice. (B) Body weights of the mice in each group. ***P<0.001. (C) Disease activity index of groups A and C. Data are presented as the mean ± SD. Group A, 10 mg/kg azoxymethane and 3% dextran sodium sulfate water; group B, 10 mg/kg azoxymethane; group C, 3% dextran sodium sulfate water; group D, blank control.

time compared with group D (blank control group; Fig. 1B). The average weight of the mice in group C declined from 21.6±1.3 g at the beginning of the experiment to 20.8±0.8 g by week 23, while the average weight of the mice in group A decreased from 21.6±1.23 g at the beginning of the experiment to 19.5±0.7 g by week 23; the differences between groups A and D, and groups C and D were statistically significant at week 23 (P<0.05). The DAI, which reflects the severity of colitis, was also markedly increased in groups A and C after DSS administration (on the 1st, 3rd and the 6th week; Fig. 1C). No weight loss or any signs of inflammation, such as loose stool or diarrhea, positive fecal occult blood or gross bleeding, were observed in groups B (AOM) and D (blank control). The DAI of groups B and D was zero throughout the modeling process and is therefore not shown in Fig. 1C. The lengths of the large bowels in groups A and C were decreased compared with groups B and D (Fig. 2A). Notably, the lengths of the large bowels were significantly decreased in groups A and C from week 3 compared with the control group (mice sacrificed in group D at week 0) or with group D(P<0.05; Fig. 2B). However, the severity of inflammation was significantly increased in group A compared with in group C at week 23, and the extent of inflammation was significantly increased in group A compared with in group C after week 18 (P<0.05), while there was no significant differences in the thickness of inflammation and the severity of epithelial damage between groups A and C (Fig. 2C).

By the 12th week, colorectal tumors were only observed in the mice of group A (Fig. 2D). Pathological results further revealed that the mice in group A presented with acute inflammation (AIF), chronic inflammation (CIF), adenoma and adenocarcinoma of the colorectum at weeks 3, 6, 12 and 18, respectively (Fig. 2D and E).

Expression levels of TLR9 and NF-κB are simultaneously upregulated during the development of chronic colitis in CRC. IHC staining revealed that TLR9 was located in the cytoplasm of the intestinal epithelial cells (IECs) and inflammatory cells in the lamina propria (Fig. 3A). TLR9 expression levels were significantly upregulated in AIF, CIF, adenoma and adenocarcinoma tissues compared with the corresponding tissues from control mice (group D; P=0.0334, P=0.0379, P=0.0437 and P=0.0008, respectively; Fig. 3B). Furthermore, the protein expression levels of TLR9 was significantly upregulated in the adenocarcinoma tissue compared with the AIF (P=0.0077), CIF (P=0.0278) and adenoma (P=0.0273) tissue (Fig. 3B).

The positive NF-κB region was mainly confined to the cytoplasm of the IECs and inflammatory cells (Fig. 3A). The IHC results revealed that the expression levels of NF-κB were significantly upregulated in the AIF, CIF, adenoma and adenocarcinoma tissues compared with the corresponding tissues from control mice (P=0.0061, P=0.0043, P=0.0019 and

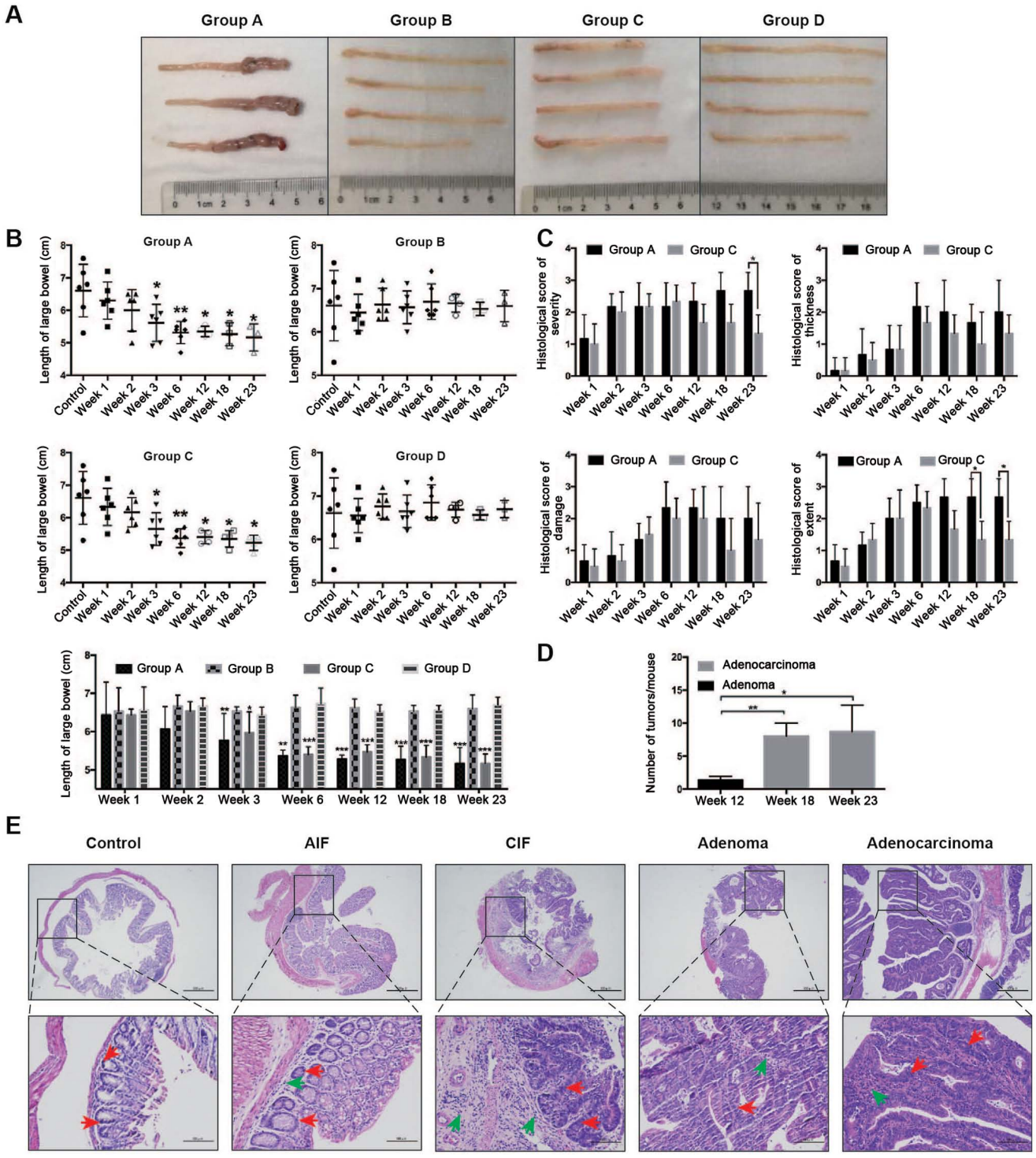

Figure 2. Colorectal pathological results in mice. (A) Length of the large bowels of mice in each group at week 18. Representative bowels from 3-4 independent animals are shown. (B) Mean length of large bowel of mice in each group. *P<0.05, **P<0.01, ***P<0.001 vs. control (mice sacrificed in group D at week 0) or group D (bottom graph). (C) Histological score of severity, thickness, damage and extent of lesions of the colorectums from mice in groups A and C. *P<0.05. (D) Large bowels were retrieved at week 12, 18 and 23 from mice in group A to determine the numbers of tumors formed. *P<0.05, **P<0.01. (E) Histological analysis of various pathological changes in the colons of mice in group A were determined using hematoxylin and eosin staining. The control groups represents tissues taken at week 0 from group D. Scale bars, 500-μm (upper) and 100-μm (lower). Inflammatory cells (green arrows) and intestinal epithelial cells (red arrows) are indicated. Group A, 10 mg/kg azoxymethane and 3% dextran sodium sulfate water; group C, 3% dextran sodium sulfate water; AIF, acute inflammation; CIF, chronic inflammation.

P<0.0001, respectively; Fig. 3D). Moreover, NF-κB expression levels were significantly upregulated in the adenocarcinoma tissue compared with the AIF (P<0.0001) and adenoma (P=0.0161) tissues (Fig. 3D).

Ki67 expression levels were observed in the nuclei of IECs and inflammatory cells (Fig. 3A). The IHC results revealed that the Ki67 expression levels were gradually upregulated across the intestinal lesions, including in the AIF, CIF, adenoma and

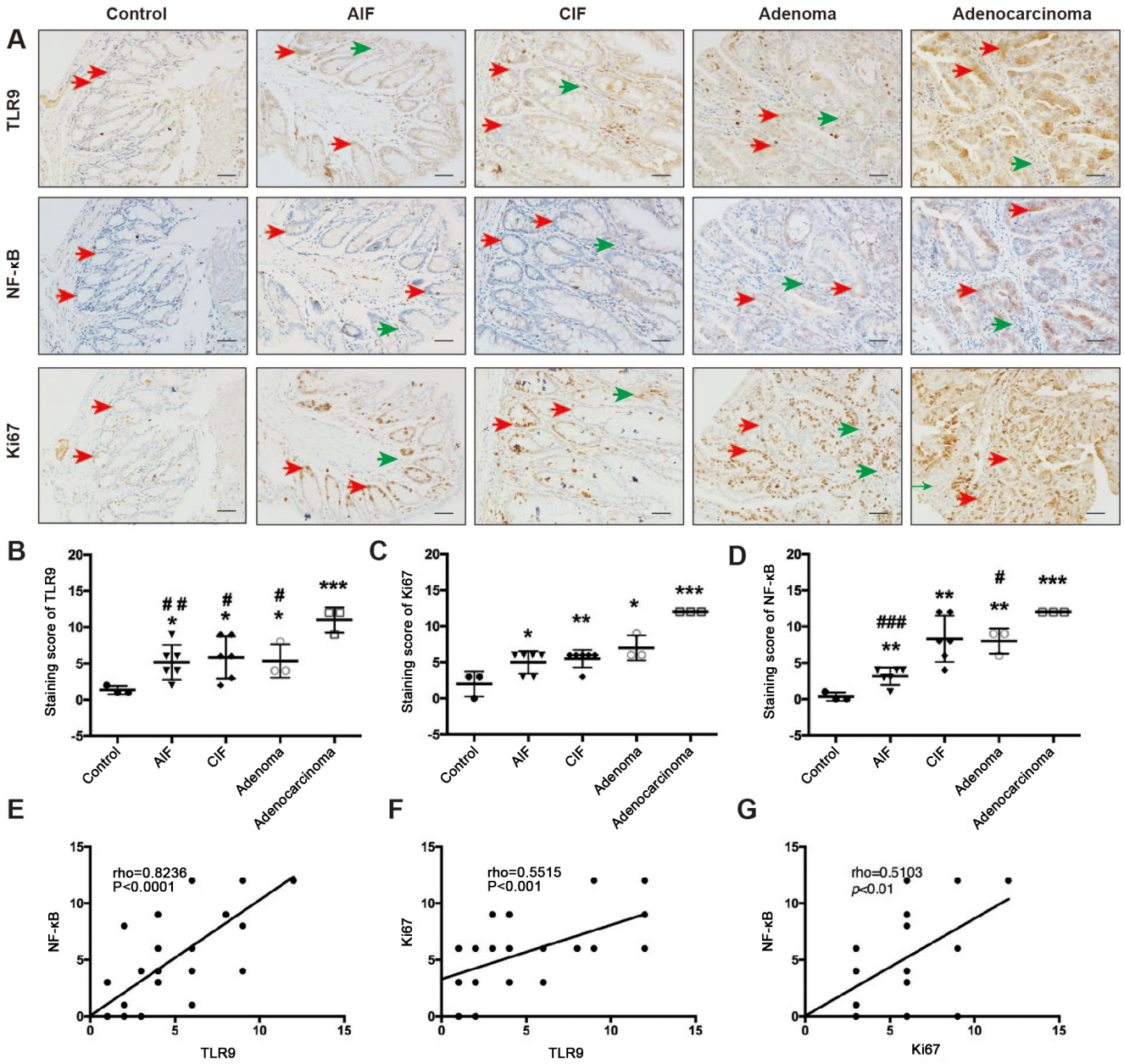

Figure 3. TLR9 and NF-κB are simultaneously upregulated as CAC develops. (A) IHC was used to analyze the expression levels and localization of TLR9, NF-κB and Ki67 in colorectal sections obtained from mice in group A. Inflammatory cells (green arrows) and intestinal epithelial cells (red arrows) are indicated. IHC staining scores of (B) TLR9, (C) Ki67 and (D) NF-κB in sections of normal control (group D), AIF, CIF, adenoma and adenocarcinoma tissues, which were obtained as described in the methods section. Scale bar, 50-μm. *P<0.05, **P<0.01 and ***P<0.001 vs. control; $^{\#}$P<0.05, $^{\#\#}$P<0.01 and $^{\#\#\#}$P<0.001 vs. adenocarcinoma. Correlation analysis of (E) TLR9 and NF-κB expression levels, (F) Ki67 and TLR9 expression levels and (G) NF-κB and Ki67 expression levels was conducted using Spearman's rank correlation. Group A, 10 mg/kg azoxymethane and 3% dextran sodium sulfate water; AIF, acute inflammation; CIF, chronic inflammation; TLR9, Toll-like receptor 9; IHC, immunohistochemistry.

adenocarcinoma tissues (P=0.0331, P=0.0092, P=0.0241 and P=0.0006, respectively) compared with the expression levels in the corresponding tissues from the control mice (Fig. 3C). Interestingly, the expression levels of TLR9 and NF-κB were discovered to be significantly positively correlated with other (rho=0.8236; P<0.0001; Fig. 3E). In addition, a significant positive correlation was also identified between TLR9 and Ki67 expression levels (rho=0.5515; P<0.001; Fig. 3F) and between NF-κB and Ki67 expression levels (rho=0.5103; P<0.01; Fig. 3G).

Downregulated TLR9 expression levels reduces the migration, viability and colony formation of HT29 cells. To further investigate the role of TLR9 in CRC, the human CRC cell line HT29 was treated with chloroquine (an inhibitor of TLR9) *in vitro*. The results revealed that suppressing TLR9 with chloroquine (at both doses) inhibited the migration, viability and colony formation ability of HT29 cells in a dose-dependent manner (Fig. 4A-E). Additionally, lysates were collected from HT29 cells treated with either different concentrations of chloroquine for 72 h or 25 μg/ml chloroquine for different time periods (Fig. 4F-I) and western blotting was performed. The analysis revealed that the expression levels of TLR9, NF-κB, PCNA, MyD88 and Bcl-xl were gradually downregulated in HT29 cells treated with increasing doses of chloroquine compared with the

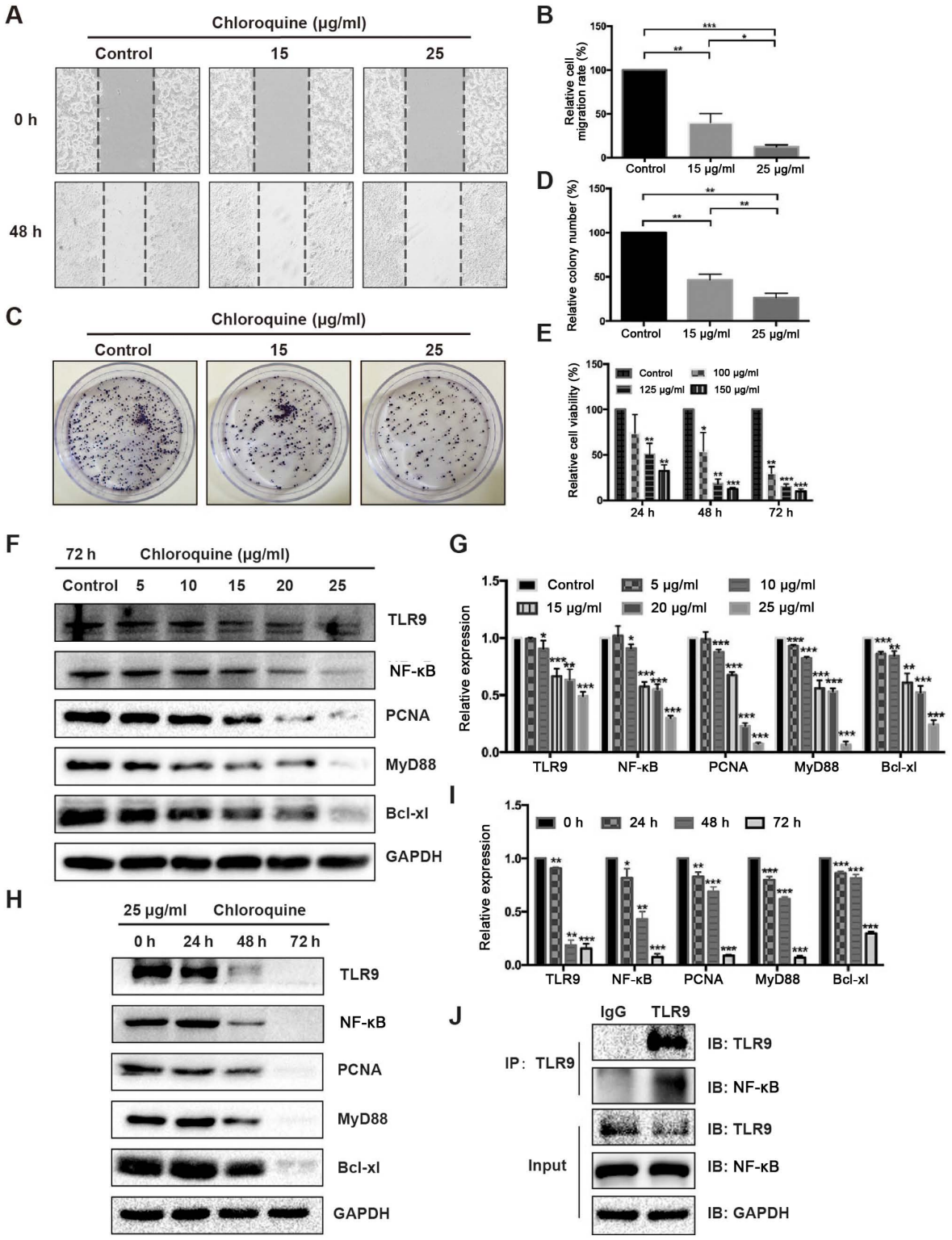

Figure 4. Chloroquine inhibits the migration, viability and colony formation of HT29 cells by inhibiting TLR9. Chloroquine (15 and 25 μg/ml) inhibited the migration of HT29 cells in a dose-dependent manner at 48 h compared with the control group, which was determined using a wound healing assay. (A) Representative images were photographed (magnification x100) and (B) migration rates were calculated. Proliferation rate of HT29 cells was reduced by chloroquine treatment (15 and 25 μg/ml), which was determined using a colony formation assay. (C) Representative images were photographed and (D) the relative colony number was analyzed. *P<0.05, **P<0.01, ***P<0.001. (E) Viability of HT29 cells was decreased by chloroquine (100, 125 and 150 μg/ml) at 24, 48 and 72 h compared with the control cells, as determined using an MTT assay. (F) Expression levels of TLR9, NF-κB, PCNA, MyD88 and Bcl-xl in lysates obtained from HT29 cells treated with numerous concentrations of chloroquine (0, 5, 10, 15, 20 or 25 μg/ml) for 72 h were analyzed using western blotting. (G) Semi-quantification of the expression levels of the proteins presented in part (F) was performed using ImageJ software. GAPDH was used as the loading control and for normalization. (H) Expression levels of TLR9, NF-κB, PCNA, MyD88 and Bcl-xl in lysates obtained from HT29 cells treated with 25 μg/ml chloroquine for numerous durations (0, 24, 48 or 72 h) were analyzed using western blotting. (I) Semi-quantification of the expression levels of the proteins presented in part (H) was performed using ImageJ software. GAPDH was used as the loading control and for normalization. (J) TLR9 interacted with the NF-κB protein in HT29 cells, which was determined using a co-immunoprecipitation assay. Goat anti-mouse IgG antibody was used as the negative control. All data are expressed as the mean ± SD of three independent experiments. *P<0.05, **P<0.01, ***P<0.001 vs. control/0 h. TLR9, Toll-like receptor 9; PCNA, proliferating cell nuclear antigen; MyD88, myeloid differentiation primary response protein MyD88; IP, immunoprecipitated; IB, immunoblotting.

control group (Fig. 4F and G). A similar trend was observed in the expression levels of these proteins as the duration of chloroquine treatment increased (Fig. 4H and I). Thus, these results indicated that the expression levels of TLR9, NF-κB, PCNA, MyD88 and Bcl-xl in HT29 cells treated with chloroquine may be downregulated in both a dose- and time-dependent manner (Fig. 4F-I). To verify whether TLR9 affected the colorectal carcinogenesis by interacting with NF-κB, co-immunoprecipitation assay was used to detect the interaction between TLR9 and NF-κB in HT-29 cells. The results revealed that there was an interaction between TLR9 and NF-κB (Fig. 4J)

Discussion

Colorectal carcinogenesis is a multi-step process, starting from normal crypts to aberrant crypt foci, then to polyps, adenoma and eventually adenocarcinoma (37,38). It has been reported that individuals with IBD may have an increased risk of developing CRC, which is directly proportional to the extent and duration of their disease (39,40). However, the exact mechanism and duration required for chronic colitis to develop into adenoma and then adenocarcinoma remains unclear (40). It has been suggested that patients with IBD have an increased risk of CRC following the inflammation-dysplasia-carcinoma model (41), including dysplasia and CRC as primary consequences of chronic inflammation. However, there are currently still no defined molecular biomarkers or existing monitoring protocols for detecting the occurrence of a malignant tumor, except for frequent colonoscopy examinations.

In the present study, an acute colitis-chronic colitis-adenoma-adenocarcinoma model was successfully constructed via AOM/DSS induction. Using this model, TLR9 expression levels were discovered to be upregulated as the severity of the colorectal lesions increased, which indicated that TLR9 protein expression levels may be continuously activated during colitis-CRC development. TLR9 is a critical protein associated with innate and acquired immunity (42), and it has been demonstrated to serve a significant role in the development of colitis (11,43) and sporadic CRC (12,13). However, the mechanism by which TLR9 regulates the development of CRC remains to be elucidated.

Interestingly, IHC analysis revealed that the expression levels of NF-κB and Ki67 were simultaneously upregulated alongside TLR9 expression levels. Notably, inhibiting TLR9 decreased the migration, proliferation and viability of HT29 cells *in vitro*, and TLR9 expression levels *in vivo* were identified to be significantly positively correlated with the expression levels of NF-κB and Ki67 (a cell proliferation marker) during the transition from colitis to CRC. The present study further revealed that the inhibition of TLR9 *in vitro* significantly downregulated the expression levels of NF-κB, MyD88, PCNA and the anti-apoptotic protein Bcl-xl in a dose- and time-dependent manner. Notably, a previous study reported that TLR9 promoted the tumor-propagating potential of prostate cancer cells via NF-κB signaling (22). Thus, the findings of the present study indicated that TLR9 may promote CAC through NF-κB signaling. However, these findings may be controversial because other previous studies have revealed that TLR9 agonists exerted an antitumor effect in CRC (14,15,44,45). The majority of these studies primarily focused on the role of TLR9 in colitis or sporadic CRC, whereas the current study focused on the role of TLR9 in the pathogenesis of CAC to provide novel targets for the treatment of CAC. For example, alterations in microtubule end-binding protein 1 were identified as a characteristic of sporadic, but not UC-associated CRC (46), and in another previous study, the immune profiling patterns of patients with CAC were significantly different compared with the patients with sporadic CRC (47).

Chloroquine, a non-specific inhibitor of TLR9, is an old antimalarial drug (48), which has recently attracted significant interest for its potential antitumor properties; for example, numerous studies have reported that chloroquine directly regulated cancer cells by inducing apoptosis, inhibiting autophagy, interacting with nucleotides, eliminating cancer stem cells and enhancing the growth of cancer cells (49-51). Chloroquine also inhibited the expression levels of TLR9 by preventing the acidification and maturation of the endosomes, and the trafficking of TLRs (52). Due to the multiple effects of chloroquine on tumor cells, different concentrations of chloroquine were selected for use in the present study based on the lowest dose according to previous studies (49,53), in order to obtain the best possible results with low toxicity to the cells. In the future, investigations using small interfering RNA targeting TLR9 should be performed to determine the effect on the biological processes of CRC cell lines to further verify the findings of the present study. Thus, our future studies will focus on investigating the precise molecular mechanism by which TLR9 participates in the early occurrence of colorectal carcinogenesis.

In conclusion, the present study developed a CAC animal model. The findings indicated that TLR9 may be closely associated with the process of inflammation-dysplasia-carcinoma and may impact carcinogenesis by regulating the NF-κB signaling pathway. These results may provide promising potential to be developed into an early detection protocol or therapeutic molecular target for CRC.

Acknowledgements

Not applicable.

Funding

The present study was supported by grants from the National Natural Science Foundation of China (grant nos. 81660404 and 81560398), the Foundation of Jiangxi Educational Committee (grant no. GJJ170016) and the Graduate Student Innovation Funding Program of Nanchang University (grant no. CX2019119).

Availability of data and materials

All data generated or analyzed during this study are included in this published article. The original data are available from the corresponding author on reasonable request.

Authors' contributions

CZ and QL designed the study and drafted the manuscript. QL and LZ performed the experiments. QL, CT and ZZ analyzed the data. QL, CZ and YC revised the manuscript for important

intellectual content. CZ and YC made substantial contributions to conception, design and coordination of the study and gave final approval of the version to be published. All authors have read and approved the final manuscript.

Ethics approval and consent to participate

All animal experiments were approved by the Ethics Committee of The First Affiliated Hospital of Nanchang University (Nanchang, China; approval no. 2015- 045).

Patient consent for publication

Not applicable.

Competing interests

The authors declare that they have no competing interests.

References

1. Bray F, Ferlay J, Soerjomataram I, Siegel RL, Torre LA and Jemal A: Global cancer statistics 2018: GLOBOCAN estimates of incidence and mortality worldwide for 36 cancers in 185 countries. CA Cancer J Clin 68: 394-424, 2018.
2. Balkwill F and Mantovani A: Inflammation and cancer: Back to virchow? Lancet 357: 539-545, 2001.
3. Eaden JA, Abrams KR and Mayberry JF: The risk of colorectal cancer in ulcerative colitis: A meta-analysis. Gut 48: 526-535, 2001.
4. Moldoveanu AC, Diculescu M and Braticevici CF: Cytokines in inflammatory bowel disease. Rom J Intern Med 53: 118-127, 2015.
5. Hemmi H, Takeuchi O, Kawai T, Kaisho T, Sato S, Sanjo H, Matsumoto M, Hoshino K, Wagner H, Takeda K and Akira S: A toll-like receptor recognizes bacterial DNA. Nature 408: 740-745, 2000.
6. Krieg AM, Yi AK, Matson S, Waldschmidt TJ, Bishop GA, Teasdale R, Koretzky GA and Klinman DM: CpG motifs in bacterial DNA trigger direct B-cell activation. Nature 374: 546-549, 1995.
7. Kolumam GA, Thomas S, Thompson LJ, Sprent J and Murali-Krishna K: Type I interferons act directly on CD8 T cells to allow clonal expansion and memory formation in response to viral infection. J Exp Med 202: 637-650, 2005.
8. Havenar-Daughton C, Kolumam GA and Murali-Krishna K: Cutting Edge:The direct action of type I IFN on CD4 T cells is critical for sustaining clonal expansion in response to a viral but not a bacterial infection. J Immunol 176: 3315-3319, 2006.
9. Akira S and Takeda K: Toll-Like receptor signaling. Nat Rev Immunol 4: 499-511, 2004.
10. Sanchez-Munoz F, Fonseca-Camarillo G, Villeda-Ramirez MA, Miranda-Pérez E, Mendivil EJ, Barreto-Zúñiga R, Uribe M, Bojalil R, Domínguez-López A and Yamamoto-Furusho JK: Transcript levels of toll-like receptors 5, 8 and 9 correlate with inflammatory activity in ulcerative colitis. BMC Gastroenterol 11: 138, 2011.
11. Fan Y and Liu B: Expression of Toll-Like receptors in the mucosa of patients with ulcerative colitis. Exp Ther Med 9: 1455-1459, 2015.
12. Eiro N, Gonzalez L, Gonzalez LO, Andicoechea A, Fernández-Díaz M, Altadill A and Vizoso FJ: Study of the expression of toll-like receptors in different histological types of colorectal polyps and their relationship with colorectal cancer. J Clin Immunol 32: 848-854, 2012.
13. Gao C, Qiao T, Zhang B, Yuan S, Zhuang X and Luo Y: TLR9 signaling activation at different stages in colorectal cancer and NF-kappaB expression. Onco Targets Ther 11: 5963-5971, 2018.
14. Nojiri K, Sugimoto K, Shiraki K, Tameda M, Inagaki Y, Kusagawa S, Ogura S, Tanaka J, Yoneda M, Yamamoto N, *et al*: The expression and function of Toll-like receptors 3 and 9 in human colon carcinoma. Oncol Rep 29: 1737-1743, 2013.
15. Shahriari S, Rezaeifard S, Moghimi HR, Khorramizadeh MR and Faghih Z: Cell membrane and intracellular expression of toll-like receptor 9 (TLR9) in colorectal cancer and breast cancer cell-lines. Cancer Biomark 18: 375-380, 2017.
16. Taniguchi K and Karin M: NF-κB, inflammation, immunity and cancer: Coming of age. Nat Rev Immunol 18: 309-324, 2018.
17. Capece D, Verzella D, Tessitore A, Alesse E, Capalbo C and Zazzeroni F: Cancer secretome and inflammation: The bright and the dark sides of NF-kappaB. Semin Cell Dev Biol 78: 51-61, 2018.
18. Said AH, Raufman JP and Xie G: The role of matrix metalloproteinases in colorectal cancer. Cancers 6: 366-375, 2014.
19. Xue Q, Cao L, Chen XY, Zhao J, Gao L, Li SZ and Fei Z: High expression of MMP9 in glioma affects cell proliferation and is associated with patient survival rates. Oncol Lett 13: 1325-1330, 2017.
20. Ha SH, Kwon KM, Park JY, Abekura F, Lee YC, Chung TW, Ha KT, Chang HW, Cho SH, Kim JK and Kim CH: Esculentoside H inhibits colon cancer cell migration and growth through suppression of MMP-9 gene expression via NF-kB signaling pathway. J Cell Biochem 120: 9810-9819, 2019.
21. Xu L, Wang C, Wen Z, Yao X, Liu Z, Li Q, Wu Z, Xu Z, Liang Y and Ren T: Selective up-regulation of CDK2 is critical for TLR9 signaling stimulated proliferation of human lung cancer cell. Immunol Lett 127: 93-99, 2010.
22. Moreira D, Zhang Q, Hossain DM, Nechaev S, Li H, Kowolik CM, D'Apuzzo M, Forman S, Jones J, Pal SK and Kortylewski M: TLR9 signaling through NF-kappaB/RELA and STAT3 promotes tumor-propagating potential of prostate cancer cells. Oncotarget 6: 17302-17313, 2015.
23. Cai Y, Huang J, Xing H, Li B, Li L, Wang X, Peng D and Chen J: Contribution of FPR and TLR9 to hypoxia-induced chemoresistance of ovarian cancer cells. Onco Targets Ther 12: 291-301, 2019.
24. Olbert PJ, Kesch C, Henrici M, Subtil FS, Honacker A, Hegele A, Hofmann R and Hänze J: TLR4- and TLR9-dependent effects on cytokines, cell viability, and invasion in human bladder cancer cells. Urol Oncol 33: e119-e127, 2015.
25. Gao C, Kozlowska A, Nechaev S, Li H, Zhang Q, Hossain DM, Kowolik CM, Chu P, Swiderski P, Diamond DJ, *et al*: TLR9 signaling in the tumor microenvironment initiates cancer recurrence after radiotherapy. Cancer Res 73: 7211-7221, 2013.
26. Tanaka T: Colorectal carcinogenesis: Review of human and experimental animal studies. J Carcinog 8: 5, 2009.
27. Zeng CY, Zhan YS, Huang J and Chen YX: MicroRNA7 suppresses human colon cancer invasion and proliferation by targeting the expression of focal adhesion kinase. Mol Med Rep 13: 1297-1303, 2016.
28. Tian Y, Xu Q, Sun L, Ye Y and Ji G: Short-Chain fatty acids administration is protective in colitis-associated colorectal cancer development. J Nutr Biochem 57: 103-109, 2018.
29. Tian Y, Wang K, Wang Z, Li N and Ji G: Chemopreventive effect of dietary glutamine on colitis-associated colon tumorigenesis in mice. Carcinogenesis 34: 1593-1600, 2013.
30. Hudert CA, Weylandt KH, Lu Y, Wang J, Hong S, Dignass A, Serhan CN and Kang JX: Transgenic mice rich in endogenous omega-3 fatty acids are protected from colitis. Proc Natl Acad Sci USA 103: 11276-11281, 2006.
31. Truelove SC and Richards WC: Biopsy studies in ulcerative colitis. Br Med J 9: 1315-1318, 1956.
32. Sangfelt P, Carlson M, Thörn M, Lööf L and Raab Y: Neutrophil and eosinophil granule proteins as markers of response to local prednisolone treatment in distal ulcerative colitis and proctitis. Am J Gastroenterol 96: 1085-1090, 2001.
33. Zeng C, Wang Y, Lu Q, Chen J, Zhang J, Liu T, Lv N, and Luo S: SPOP suppresses tumorigenesis by regulating Hedgehog/Gli2 signaling pathway in gastric cancer. J Exp Clin Cancer Res 33: 75, 2014.
34. Scharl A, Vierbuchen M, Conradt B, Moll W, Würz H and Bolte A: Immunohistochemical detection of progesterone receptor in formalin-fixed and paraffin-embedded breast cancer tissue using a monoclonal antibody. Arch Gynecol Obstet 247: 63-71, 1990.
35. Pan X, Zhou T, Tai YH, Wang C, Zhao J, Cao Y, Chen Y, Zhang PJ, Yu M, Zhen C, *et al*: Elevated expression of CUEDC2 protein confers endocrine resistance in breast cancer. Nat Med 17: 708-714, 2011.
36. Remmele W and Stegner HE: Recommendation for uniform definition of an immunoreactive score (IRS) for immunohistochemical estrogen receptor detection (ER-ICA) in breast cancer tissue. Pathologe 8: 138-140, 1987.

37. Kinzler KW and Vogelstein B: Lessons from hereditary colorectal cancer. Cell 87: 159-170, 1996.
38. Brenner H, Kloor M and Pox CP: Colorectal cancer. Lancet 383: 1490-1502, 2014.
39. Beaugerie L and Itzkowitz SH: Cancers complicating inflammatory bowel disease. N Engl J Med 372: 1441-1452, 2015.
40. Terzić J, Grivennikov S, Karin E and Karin M: Inflammation and colon cancer. Gastroenterology 138: 2101-2114, 2010.
41. Itzkowitz SH and Yio X: Inflammation and cancer IV. Colorectal cancer in inflammatory bowel disease: The role of inflammation. Am J Physiol Gastrointest Liver Physiol 287: G7-G17, 2004.
42. Akira S, Takeda K and Kaisho T: Toll-Like receptors: Critical proteins linking innate and acquired immunity. Nat Immunol 2: 675-680, 2001.
43. Atreya R, Bloom S, Scaldaferri F, Gerardi V, Admyre C, Karlsson Å, Knittel T, Kowalski J, Lukas M, Löfberg R, *et al*: Clinical effects of a topically applied toll-like receptor 9 agonist in active moderate-to-severe ulcerative colitis. J Crohn's Colitis 10: 1294-1302, 2016.
44. Schmoll HJ, Wittig B, Arnold D, Riera-Knorrenschild J, Nitsche D, Kroening H, Mayer F, Andel J, Ziebermayr R and Scheithauer W: Maintenance treatment with the immunomodulator MGN1703, a Toll-like receptor 9 (TLR9) agonist, in patients with metastatic colorectal carcinoma and disease control after chemotherapy: A randomised, double-blind, placebo-controlled trial. J Cancer Res Clin Oncol 140: 1615-1624, 2014.
45. Dong T, Yi T, Yang M, Lin S, Li W, Xu X, Hu J, Jia L, Hong X and Niu W: Co-Operation of alpha-galactosylceramide-loaded tumour cells and TLR9 agonists induce potent anti-tumour responses in a murine colon cancer model. Biochem J 473: 7-19, 2016.
46. Gemoll T, Kollbeck SL, Karstens KF, Hò GG, Hartwig S, Strohkamp S, Schillo K, Thorns C, Oberländer M, Kalies K, *et al*: EB1 protein alteration characterizes sporadic but not ulcerative colitis associated colorectal cancer. Oncotarget 8: 54939-54950, 2017.
47. Soh JS, Jo SI, Lee H, Do EJ, Hwang SW, Park SH, Ye BD, Byeon JS, Yang SK, Kim JH, *et al*: Immunoprofiling of colitis-associated and sporadic colorectal cancer and its clinical significance. Sci Rep 9: 6833, 2019.
48. Kuznik A, Bencina M, Svajger U, Jeras M, Rozman B and Jerala R: Mechanism of endosomal TLR inhibition by antimalarial drugs and imidazoquinolines. J Immunol 186: 4794-4804, 2011.
49. Pascolo S: Time to use a dose of chloroquine as an adjuvant to anti-cancer chemotherapies. Eur J Pharmacol 771: 139-144, 2016.
50. Maes H, Kuchnio A, Carmeliet P and Agostinis P: Chloroquine anticancer activity is mediated by autophagy-independent effects on the tumor vasculature. Mol Cell Oncol 3: e970097, 2016.
51. Lin YC, Lin JF, Wen SI, Yang SC, Tsai TF, Chen HE, Chou KY and Hwang TI: Chloroquine and hydroxychloroquine inhibit bladder cancer cell growth by targeting basal autophagy and enhancing apoptosis. Kaohsiung J Med Sci 33: 215-223, 2017.
52. Mohamed FE, Al-Jehani RM, Minogue SS, Andreola F, Winstanley A, Damink SW, Habtesion A, Malagó M, Davies N, Luong TV, *et al*: Effect of toll-like receptor 7 and 9 targeted therapy to prevent the development of hepatocellular carcinoma. Liver Int 35: 1063-1076, 2015.
53. Zhang Y, Li Y, Li Y, Ma Y, Wang H and Wang Y: Chloroquine inhibits MGC803 gastric cancer cell migration via the Toll-like receptor 9/nuclear factor kappa B signaling pathway. Mol Med Rep 11: 1366-1371, 2015.